Electronic Supporting Information

Capillary Uptake in Macroporous Compressible Sponges

Soumyajyoti Chatterjee[a,b], Pankaj Doshi[c*] and Guruswamy Kumaraswamy[a,b*]

[a]J-101, Polymers and Advanced Materials Laboratory, Complex Fluids and Polymer Engineering, Polymer Science and Engineering Division, CSIR-National Chemical Laboratory, Pune-411008, Maharashtra, India.

[b]Academy of Scientific and Innovative Research, (AcSIR), New Delhi 110025, India

[c]Pfizer, Inc., Eastern Point Road, Groton, Connecticut 06340, United States.

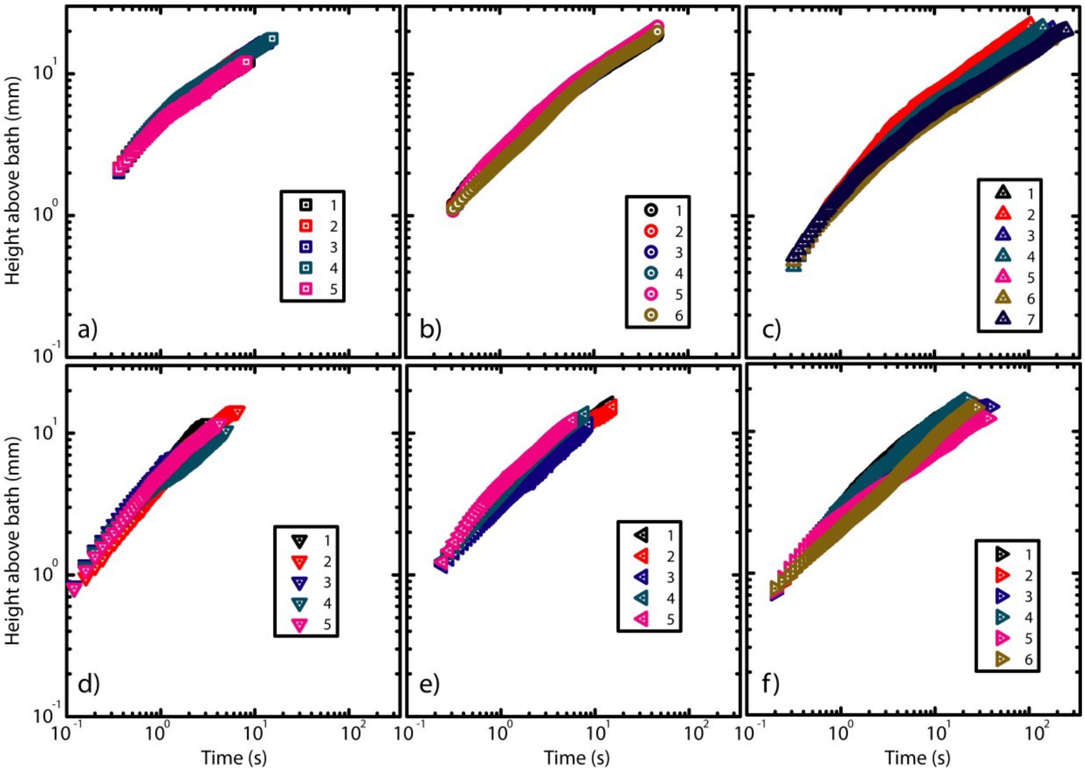

Fig. S1 Plot of capillary rise height of water above the water bath for a) S10, b) S20, (c) S30, (d) Sp3, (e) Sp7 and (f) Sp10 sponges respectively with at least 5 repetition.

Video S1: Video of capillary rise of water in the sponge.

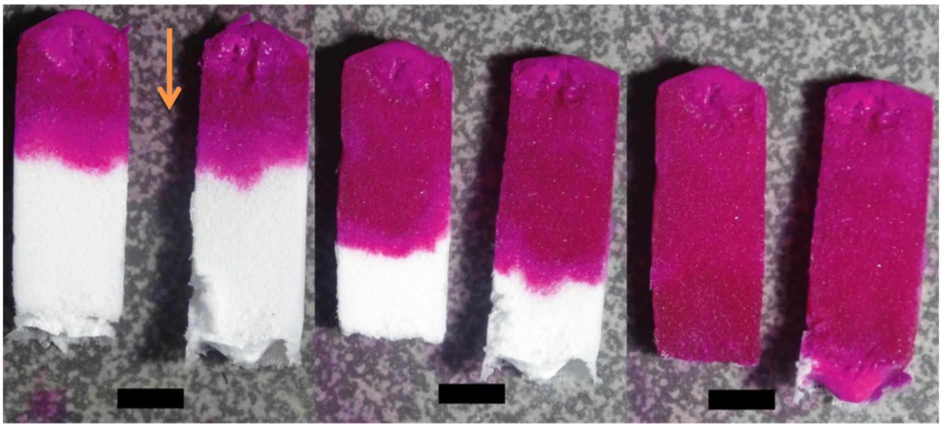

Fig. S2 Images of sponges at various stage of capillary rise experiment. Arrow attributes flow direction. Scale bars in the photographs correspond to 5 mm.

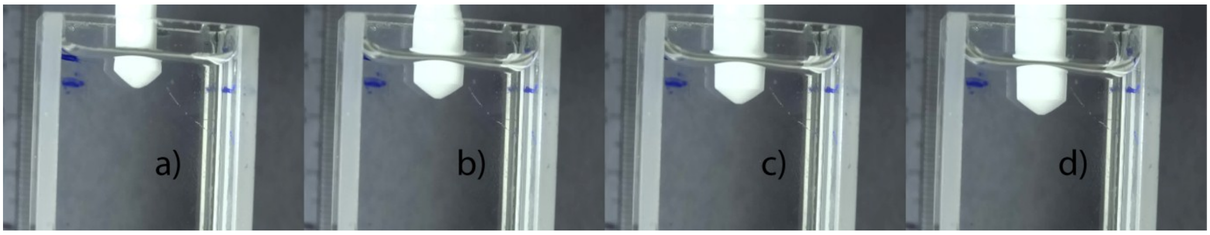

Fig. S3 Images of axial growth of the sponge inside the reservoir of Sp10 with time, as the sponge swells when water is imbibed by it: a) t=0 s, b) t=4 s, c) t=8 s and d) t=12s

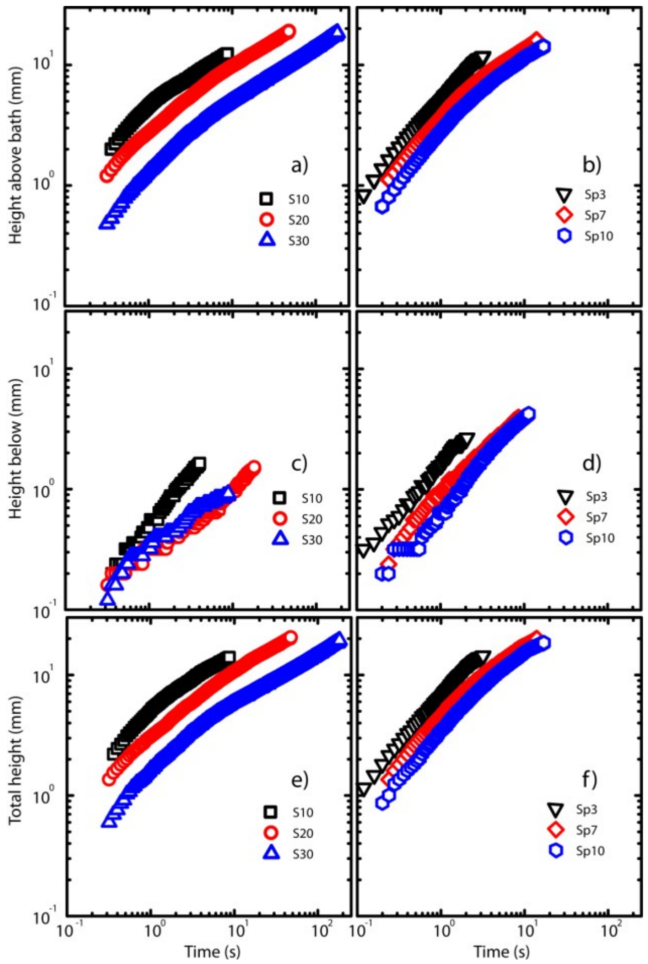

Fig. S4 Plot of capillary rise height of water above the water bath for a) composite and b) polymeric sponges. Axial growth of composite and polymeric sponges inside the water reservoir are shown in the panel c) and d) respectively. e) and f) show the total length of the sponge that has imbibed water for composite and polymeric sponges respectively.

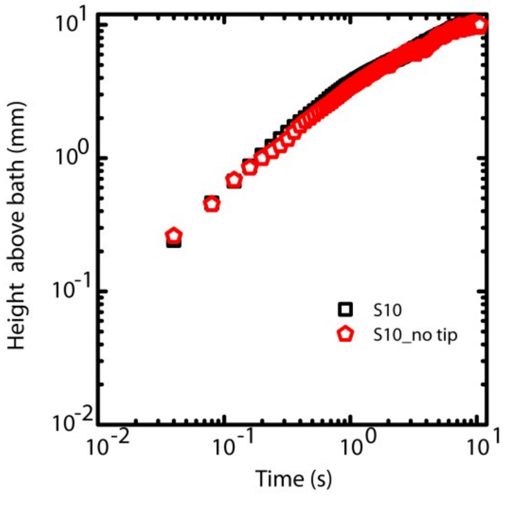

Fig. S5 Comparison of capillary rise behaviour for S10 with and without the conical geometry.

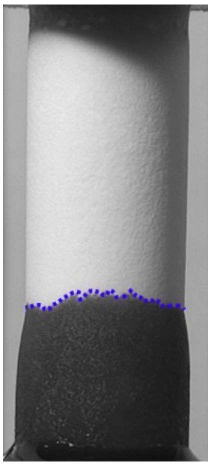

Fig. S6 The jagged growth front of the colored water front, as it propagates, is averaged and the height of this growth front from the water surface is determined. Here, the front is shown as a blue dotted line.

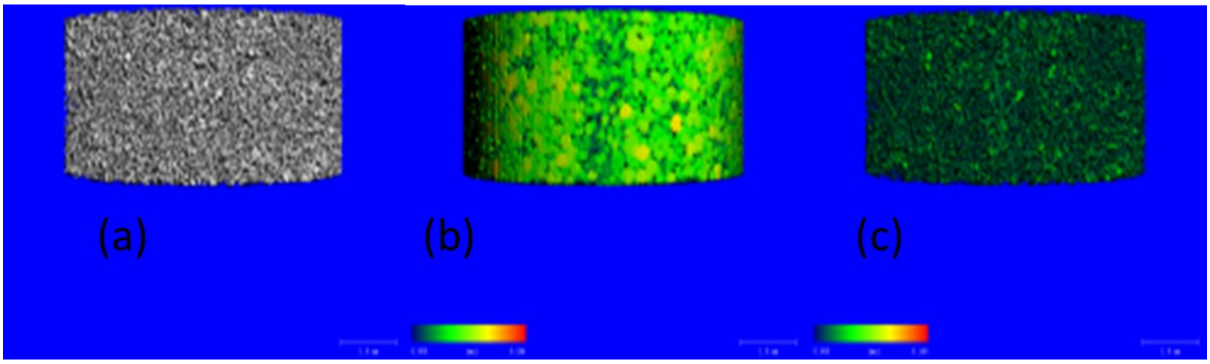

Fig. S7 Typical X-ray μ-CT images use to estimate pore size distribution, wall thickness and porosity of sponges. False color is used to render (a) the sponge; (b) the pores and (c) the walls. Colour coding represents length scale of pores and wall thickness for (b) and (c) respectively.

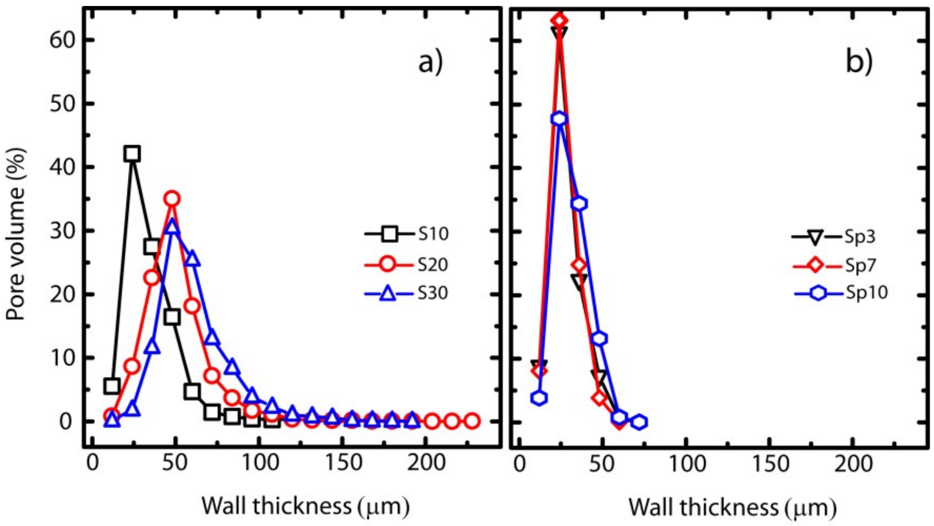

Fig. S8 Peak pore wall thickness for a) composite and b) polymeric sponges.

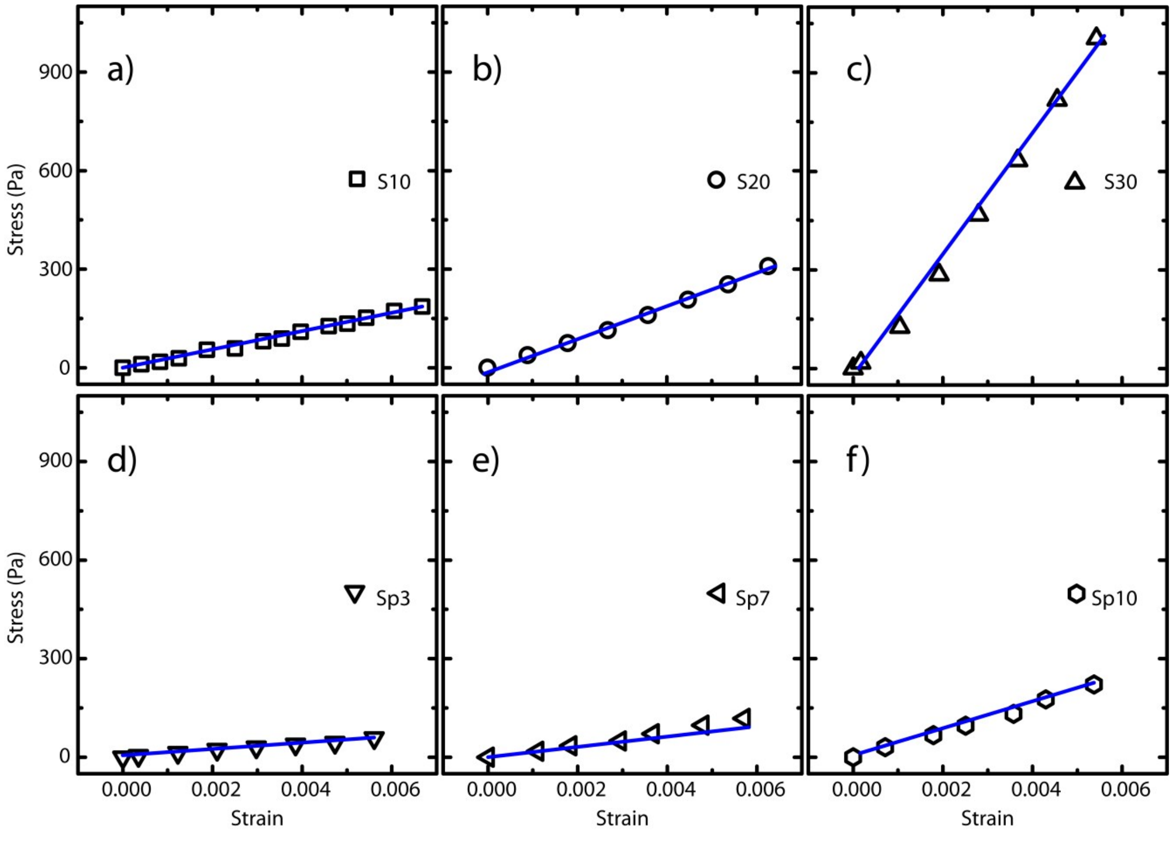

Fig. S9 Stress-strain data from compression tests on (a – c) composite sponges and (d – f) polymer sponges at very low values of strain.

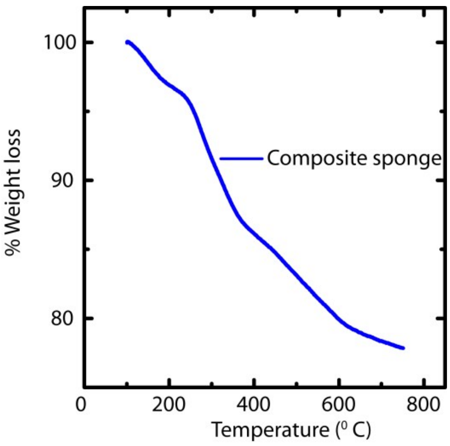

Fig. S10 TGA for S10, that is typical of data obtained for composite sponges. We have previously reported (Rajamanickam, R.; Kumari, S.; Kumar, D.; Ghosh, S.; Kim, J. C.; Tae, G.; Sen Gupta, S.; Kumaraswamy, G. Soft Colloidal Scaffolds Capable of Elastic Recovery after Large Compressive Strains. *Chem. Mater.* **2014**, *26*, 5161–5168) TGA for the silica particles, indicating a weight loss of about 5% for the neat particles. We obtain the total organic content from the TGA weight loss between 125^{o}C and 600^{o}C for the composite sponges, after accounting for the weight loss of the silica particles.

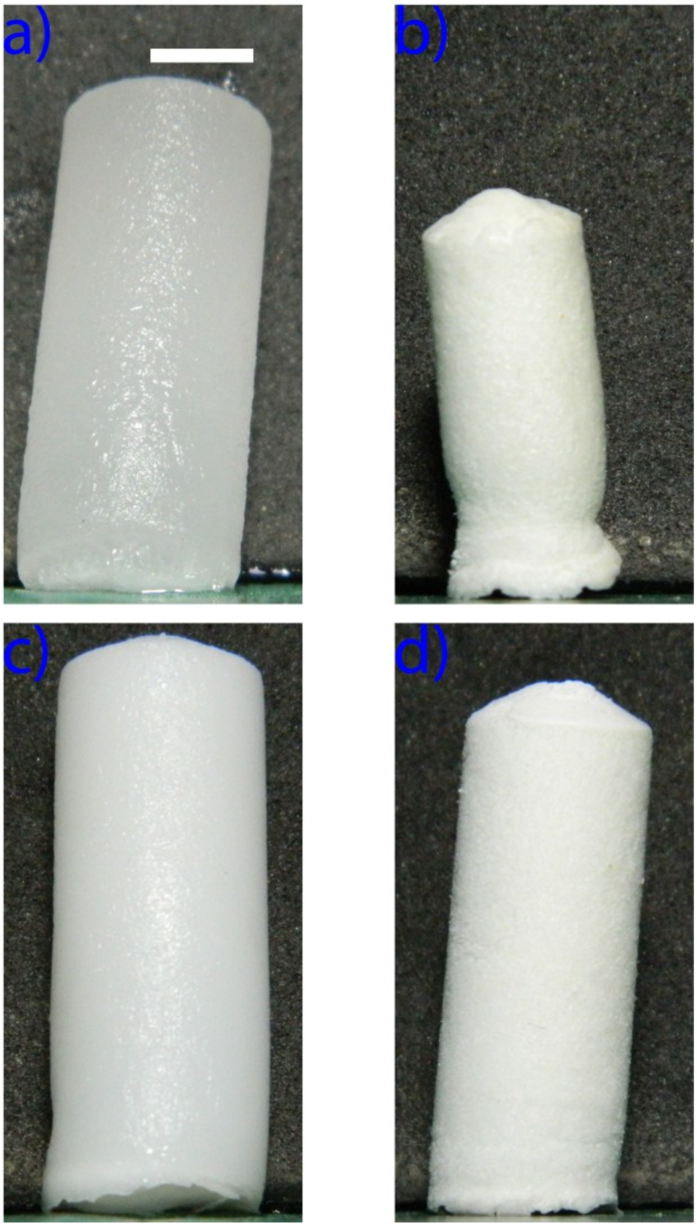

Fig. S11 Photographs of polymeric sponge, Sp3 in (a) water swollen wet state and (b) in the dry state, after air drying. The polymer sponge shows large shrinkage after air drying. In contrast, there is significantly lesser shrinkage of composite sponges (S10 as an example) as they are air dried from the (c) water swollen wet state to (d) a dry state. The scale bar in (a) represents 5 mm and applies to all photographs.

Preparation of thin films of cross-linked PEI on glass slide:

Prior to prepare thin films of cross-linked PEI, glass slides were first cleaned by treatment with piranha solution and followed by water and ethanol. The glass slides were subsequently dried in oven. The cleaned glass slides were then dip coated with different concentration of PEI/cross-linker solution to cross-link and thereafter thoroughly dried to prepare thin films of Sp10, Sp7 and Sp3.

Preparation of composite films of silica particles with cross-linked PEI on glass slide:

Prior to prepare composite thin films, glass slides were first cleaned by treatment with piranha solution and followed by water and ethanol. The glass slides were subsequently dried in oven. The cleaned glass slides were then dip coated with different concentration of PEI-coated silica particle/cross-linker solution and thereafter thoroughly dried to prepare thin films of S10, Sp20 and S30.

Measurement of contact angle on glass substrate coated with the films:

A 10 µl of dyed water droplet was gently placed on the thin film coated glass surface and video record with a home build imaging set up. Subsequently the contact angle was measured from the video extracted images using dataphysics software.

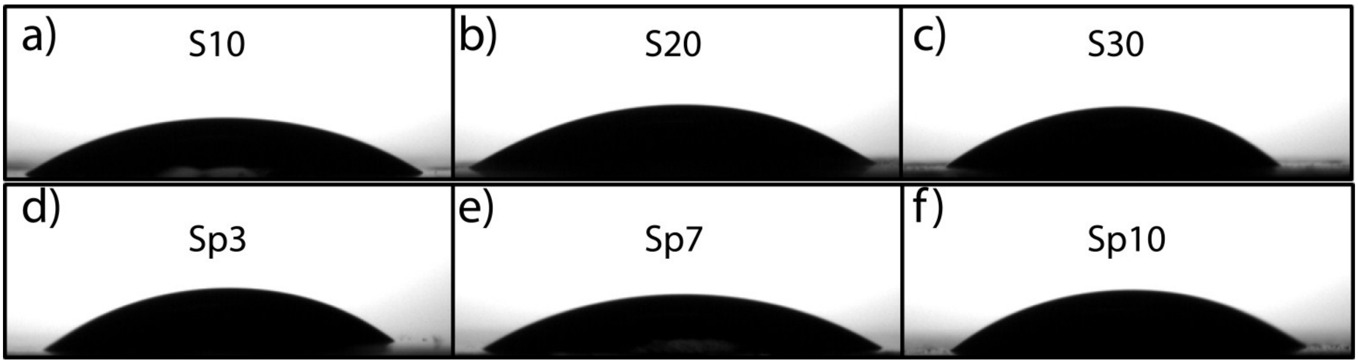

Fig. S12 Contact angle images.

Table S1

Change in dimensions on swelling of sponges. Δd is the change in diameter from the initial dry diameter, d. Δ **l** is the change in length where **l** is the dry length.

Sponge	**Change in sponge size when it is fully immersed in water**		**Water imbibition through capillary rise**	
	Vernier scale		**Image analysis**	
	Δd/d	Δ **l** / **l**	Δd/d	Δ **l** / **l**
S10	0.09	0.05	0.12	0.08
S20	0.10	0.07	0.10	0.11
S30	0.11	0.03	0.10	0.09
Sp3	0.17	0.18	0.20	0.24
Sp7	0.18	0.16	0.22	0.22
Sp10	0.17	0.17	0.23	0.25

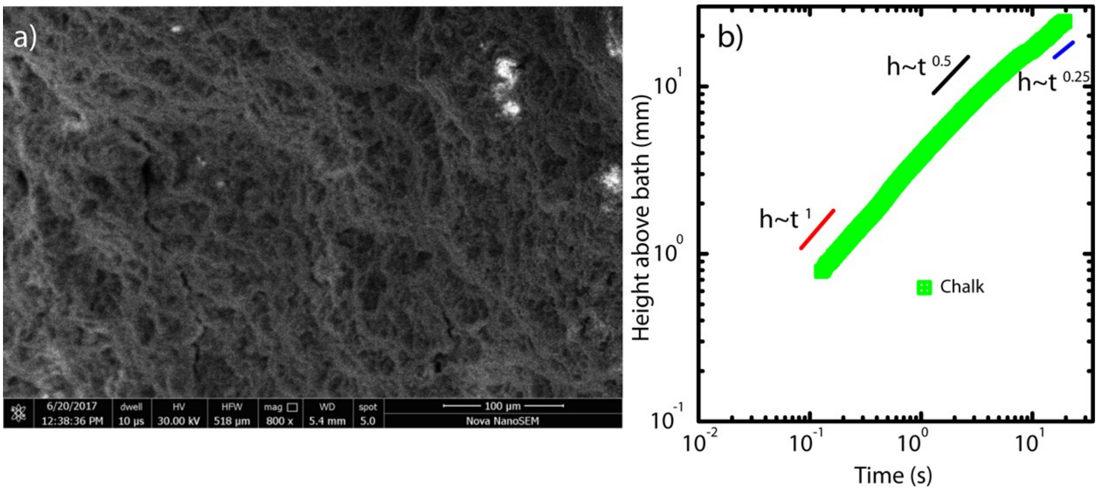

Fig. S13 (a) SEM image of chalk and (b) Capillary rise experiment using chalk, a rigid porous material. We observe inertial-capillary ($h \sim t^{1}$) and Washburn ($h \sim t^{0.5}$) regimes and observe the transition to the post- Washburn regime ($h \sim t^{0.25}$).